EDGE CONDUCTION IN VACUUM GLAZING

Tom M. Simko **Richard E. Collins**

Fredric A. Beck **Dariush Arasteh, P.E.**
Member ASHRAE

ABSTRACT

Vacuum glazing is a form of low-conductance double glazing using an internal vacuum between the two glass sheets to eliminate heat transport by gas conduction and convection. An array of small support pillars separates the sheets; fused solder glass forms the edge seal. Heat transfer through the glazing occurs by radiation across the vacuum gap, conduction through the support pillars, and conduction through the bonded edge seal. Edge conduction is problematic because it affects stresses in the edge region, leading to possible failure of the glazing; in addition, excessive heat transfer because of thermal bridging in the edge region can lower overall window thermal performance and decrease resistance to condensation.

Infrared thermography was used to analyze the thermal performance of prototype vacuum glazings, and, for comparison, atmospheric pressure superwindows. Research focused on mitigating the edge effects of vacuum glazings through the use of insulating trim, recessed edges, and framing materials. Experimentally validated finite-element and finite-difference modeling tools were used for thermal analysis of prototype vacuum glazing units and complete windows. Experimental measurements of edge conduction using infrared imaging were found to be in good agreement with finite-element modeling results for a given set of conditions. Finite-element modeling validates an analytic model developed for edge conduction.

INTRODUCTION

Heat transfer through windows is a significant source of energy loss and gain in buildings, especially in very cold or very warm climates. Heating and cooling energy lost through windows in the residential sector accounts for 3% of total U.S. energy use, costing more than $26 billion annually in energy bills (Frost et. al. 1993). The traditional approach to reducing heat transfer is to use double or multiple glazings, often with low-emissivity (low-e) coatings on the internal glass surfaces and interpane gases of low thermal conductivity. These devices can achieve a low air-to-air thermal transmittance, or U-factor. For example, argon-filled double glazing with two coatings of emissivity of 0.1 can have a center-of-glass, air-to-air U-factor as low as 1.3 $W/m^2 \cdot K$ (0.23 $Btu/h \cdot ft^2 \cdot °F$). The use of multiple glazings with three or more transparent sheets, low-emittance coatings, and gases with even lower thermal conductivity, (such as krypton or xenon) can yield values below 1.0 $W/m^2 \cdot K$ (0.18 $Btu/h \cdot ft^2 \cdot °F$). Comparable insulation performance can be achieved by evacuating the space between two sheets of glass to less than 0.1 Pa to eliminate the heat transport resulting from interpane gas conduction and convection—essentially creating a flat, transparent Dewar flask. Vacuum glazing is based upon this principle.

Vacuum glazings can be used not only for windows in cold climates, but also in doors for display refrigerators or freezers such as those found in supermarkets, and in renovation of old buildings, for which heritage listings might prohibit redesign of window frames to accommodate thicker, conventional insulating glazings. A detailed estimation of the manufacturing cost for vacuum glazing (Garrison and Collins 1995) shows that the cost is likely to be 15% greater than that of standard double glazing of similar thermal performance. The concept of vacuum glazing was first proposed in a patent application by Zoller in 1913 (Zoller 1924), 20 years after the invention of the Dewar flask. Zoller identified one of the essential features of flat vacuum glazing—a multiplicity

Tom M. Simko and **Richard E. Collins** are members of the Department of Applied Physics, School of Physics, University of Sydney, NSW, Australia. **Fredric A. Beck** and **Dariush Arasteh** are with the Energy and Environment Division,

of "ribs, grooves, prisms or projections" that keep the glass sheets apart despite atmospheric pressure. Since 1913, many other proposals have been made; none resulted in a referenced scientific report of the successful manufacture of a flat vacuum glazing until Robinson and Collins (1989) solved some of the inherent problems in the design and production of vacuum glazing.

In their design, the glass sheets are separated by an array of support pillars, and a band of solder glass around the edge makes a leak-free hermetic seal. The internal vacuum has been shown to be stable over a period of several years (Simko et al. 1995). This edge seal is a thermal bridge between the otherwise thermally isolated glass sheets, which degrades the thermal performance of the unit. Conduction through the glazing edge seal results in warm-side glass surface temperatures at and near the edge seal that are lower than the center-of-glass temperature. For conventional glazings, the lower temperature usually is confined to a region within 63.5 mm (2.5 in.) of the glazing sightline. This region is known as the *edge-of-glass region*, and the effect of conduction through the edge seal commonly is referred to as the *edge effect*.

Using infrared thermography and computer modeling, this paper analyzes the heat flows associated with the edge seal in vacuum glazing. A simple analytic model that gives insight into the physical processes responsible for edge conduction is presented and solved numerically. The glazing system also is analyzed using a finite-element model (FEM).

VACUUM GLAZING TECHNOLOGY

As shown in Figure 1, vacuum glazing consists of two sheets of glass separated by a narrow vacuum space, typically 0.1 to 0.2 mm in width (Collins et al. 1992). The sheets are separated by an array of small cylindrical ceramic (alumina) or metal support pillars, each about 0.25 mm in diameter. The hermetic edge seal is made with solder glass fused in place by baking the entire structure at about 500 °C (932 °F). The glazing is evacuated to less than 0.1 Pa via a small pump-out tube incorporated into one of the glass sheets, and the tube is fused shut when the evacuation process is complete. Typically, one or both inner surfaces have a low-emissivity coating to reduce interpane radiative heat transfer. With both surfaces coated with doped tin oxide, an overall air-to-air, center-of-glass U-factor as low as 0.9 $W/m^2 \cdot K$ (0.16 $Btu/h \cdot ft^2 \cdot °F$) has been measured. About 60% of the heat flow between the glass sheets is due to radiation and the remainder is due to pillar conduction. The edge seal is a thermal short circuit around the periphery that can substantially increase the heat transport through the glazing, thus degrading the overall thermal performance of the unit and decreasing condensation resistance.

In the presence of a temperature differential across the glazing, heat is conducted along the warm-side sheet, through the edge seal, and along the cold-side sheet. Edge conduction is more than just a mode of heat loss that detracts from the insulating quality of the glazing. The temperature nonuniformities associated with edge conduction can affect stresses significantly in the edge region, leading to failure of the glazing (Fisher-Cripps et al. 1995).

A temperature difference between the two glass sheets in vacuum glazing results in differential expansion of the sheets. This causes shear forces at the bonded edge seal, which result in bending of the structure and consequent stresses. Stresses in the edge region are affected by edge conduction in two ways. First, as a result of edge conduction, the temperature of the glass sheets close to the edge seal is different from the center-of-glass value; the glass is cooler near the edge on the warm side and warmer on the cold side. The spatial dependence of the glass temperature on each side depends upon both the external and internal heat transfer coefficients and upon the amount of insulation near the edge seal. These temperature nonuniformities decrease the amount of bending of the glazing because they reduce the average temperature difference between the two sides. This effect reduces the magnitude of the stresses throughout the glazing (Fisher-Cripps et al. 1995).

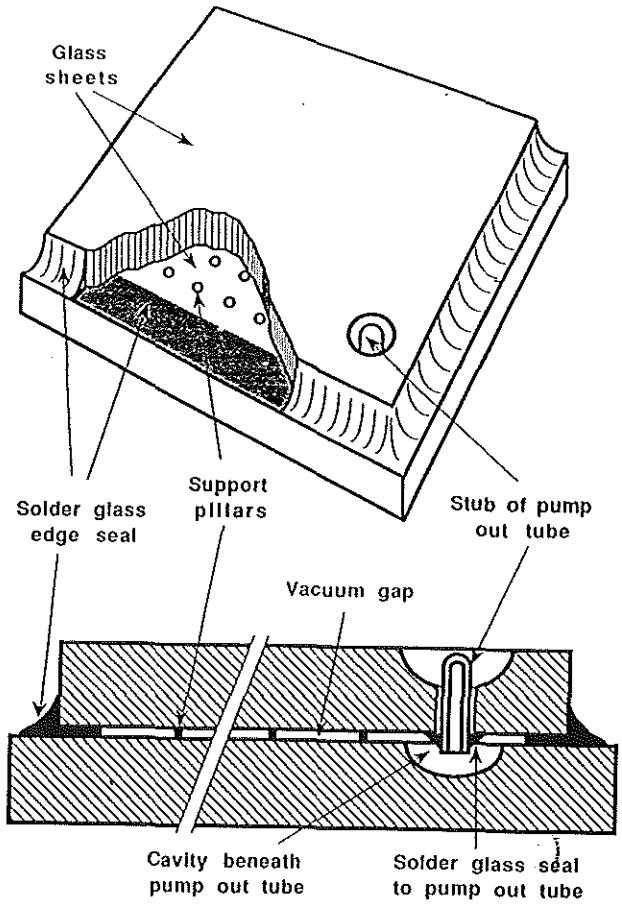

Figure 1 *Schematic diagram of the vacuum glazing specimen.*

The second stress-related effect of edge conduction results from the difference between the temperature of the bonded edge seal and the rest of the window. If the midplane temperature of the edge seal is greater or less than the mean temperature of the two glass sheets, then additional temperature-difference-dependent compressive or tensile stresses, respectively, exist in the edge seal. These stresses are directed parallel to the edge. Temperature differences of this kind can arise if the external heat transfer coefficients at the surfaces of the glass plates are unequal or because of the presence of edge insulation (Fisher-Cripps et al. 1995). A discussion of these stresses is not covered in this paper.

INFRARED THERMOGRAPHIC MEASUREMENTS

Infrared thermography is a noninvasive method for measuring surface temperatures of fenestration products in a laboratory (Arasteh et al. 1992). Thermographic tests were performed to compare vacuum glazing to conventional glazings of high thermal performance, to explore methods to mitigate heat transfer through the vacuum glazing edge, and to validate the analytical and FEM computer modeling for a number of edge configurations. The thermographic tests were carried out on a 0.5-m by 0.5-m specimen of vacuum glazing supplied by an Australian university. The glass-to-glass gap conductance (Collins et al. 1993) of this specimen was 1.1 $W/m^2 K$ (0.19 $Btu/h \cdot ft^2 \cdot °F$). The vacuum glazing was mounted in an insulating mask wall and placed between a warm box and a cold box having fixed temperature setpoints, thus creating steady-state heat transfer through the specimen after thermal equilibrium has been reached. The cold box is set at −17.8 ℃ (0.0 ℉), with an airflow of 3.6 m/s (8.0 mph) directed parallel to the glazing surface. The warm box is set at 21.1 ℃ (70.0 ℉), with natural convective airflow across the sample. A low wind speed (< 0.3 m/s [0.6 mph]) is employed in the warm box to reduce vertical temperature gradients within the enclosed air volume.

An infrared (IR) imaging radiometer linked to a computer is used to measure the warm-side surface temperature of the glazing. Reference emitter techniques and averaging of multiple images result in an estimated accuracy of 0.5 ℃ (0.9 ℉) for the surface temperature measurements. Details of the reference emitter techniques and the issues associated with the accuracy of the thermographic techniques employed in these tests appear in Griffith et al. (1995). A calibrated transfer standard (CTS) was used to measure the warm- and cold-side heat transfer coefficients for the test conditions. These surface heat transfer coefficients were determined using standard fenestration test procedures (ASTM 1991) and were used in the FEM modeling for results to be compared with the thermographic measurements. The measured heat transfer coefficients were 8.4 and 20.0 $W/m^2 K$ on the warm and cold sides, respectively.

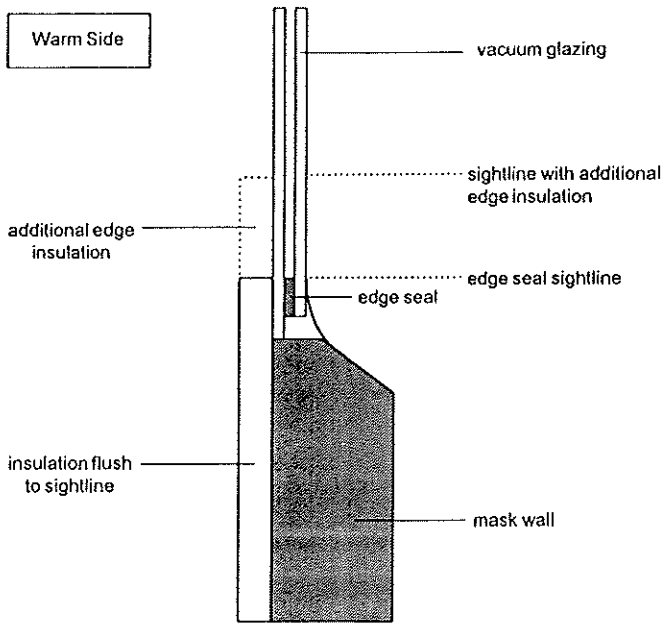

Figure 2 *Comparison of horizontal edge temperatures: vacuum glazing and superwindow.*

The edge seal of this glazing was approximately 6 mm wide. All thermographic data presented here are horizontal temperature profiles taken at the midheight of the jamb, unless otherwise noted.

Comparison to Conventional Superglazings

The vacuum glazing and a conventional glazing with similar center-of-glass U-factors were tested to compare the edge effects in vacuum glazings with those of commercially available high-thermal-performance fenestration products. The vacuum glazing was mounted in an 18 mm (0.75 in.) thick polystyrene foam mask wall, flush to the warm side.

The comparison glazing was a commercially available atmospheric pressure superwindow-type glazing: a 2.54 cm (1.0 in.) thick four-layer glazing consisting of two low-emissivity thin films (one of which was coated on both sides) suspended between two glass sheets, all glazing cavities filled with krypton gas mixture, and the edge sealed with a thermally broken spacer. A simulation (LBL 1992) predicts that this superwindow has a center-of-glass U-factor of 0.57 $W/m^2 K$ (0.10 $Btu/h \cdot ft^2 \cdot °F$). Figure 2 shows center-of-glass superwindow temperatures approximately 2 °C higher than those of the vacuum unit and sightline temperatures approximately 3°C above those of the vacuum unit. These glazings were mounted flush to both the warm and cold sides of the mask wall. While more pronounced in vacuum units, this graph highlights the significance of edge effects in both units.

Mitigation of Edge Effects and Validation of Computer Models

Successful reduction of edge effects in vacuum glazings will lead to higher warm-side edge-of-glass temperatures, resulting in increased condensation resistance, lower total window U-factors and, possibly, reduced mechanical stress. Significant edge effects are present in vacuum glazings because of the high conductance of the solder glass edge seal (in contrast to the gap conductance) and the short conductive path through the edge seal as dictated by the minimal gap between the panes of the vacuum glazing. Lengthening the conductive path between the warm- and cold-side environmental conditions at the edge is one way to reduce edge-of-glass heat transfer. Lengthening the conductive path between the warm and cold sides entails covering the edge to some degree with an insulating material or recessing the edge within a low-conductance frame deeper than standard industry practice. The mitigation of edge effects in a frame made of a material of high thermal conductance such as nonthermally broken aluminum is most likely not worthwhile, as the heat transfer through such a frame will be equal to or greater than that through the glazing edge (Byers and Arasteh 1990).

Infrared thermography was used to evaluate the reduction of edge effects in vacuum glazings achievable by (1) adding an insulating layer that extends past the edge-seal sightline on the warm-side surface, (2) recessing the glazing edge into the sash of a wood frame, and (3) adding a wood-spaced third pane to the sash, completely covering the vacuum glazing. Analytic and FEM models were used to model cases in which an insulating layer was extended past the edge seal. Modeling results were compared to IR data for the corresponding configurations. Modeling techniques are discussed in greater detail in the section on modeling.

Insulated Edge Configurations

To test the effect of an insulating edge, the evacuated glazing was mounted in an insulating foam mask wall and the edge seal covered with an insulating polystyrene foam strip on the warm-side surface, as shown in Figure 3. In these tests the insulating strips were extended past the sightline of the glazing edge seal, toward the center-of-glass region. The glazing was tested with the insulating strips in four different configurations: flush to the edge-seal sightline, and extended 0.63 cm (0.25 in.), 1.27 cm (0.50 in.), and 2.54 cm (1.0 in.) past the edge-seal sightline.

Temperature profiles for these four tests are plotted in Figure 4 along with modeling data for the same configurations. The plots show excellent agreement between the FEM and IR experimental data, which constitutes experimental validation of the ability of the model to predict the effects of edge conduction accurately. As shown in

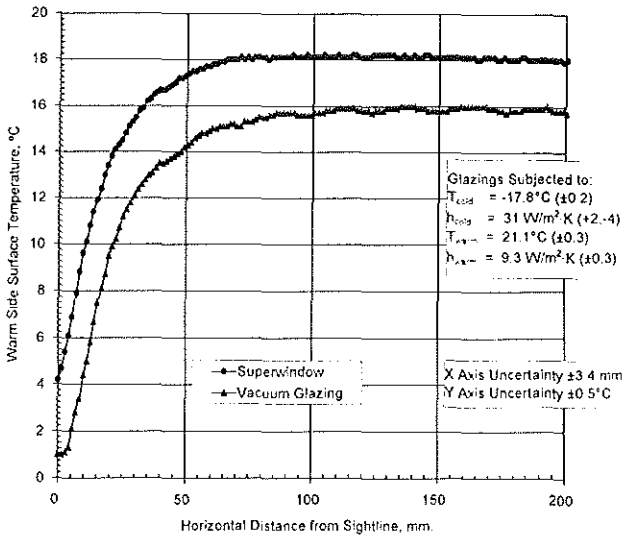

Figure 3 *Cross sectional schematic of the vacuum glazing edge-of-glass region as mounted for infrared thermographic testing*

Figure 4, the warm-side glazing sightline temperature increases by 2.5 C for the first increment of insulation of 0.63 cm, and by an additional 2.0 C for the second increment of 0.63 cm; the final increase of 2.3 C requires an additional 1.27 cm of insulation. Although these figures do not indicate the optimum amount of insulation, they show that a diminishing point of return is reached as the edge temperature gets closer to the center-of-glass temperature; one must add significantly more insulation to obtain a fixed increment of edge temperature increase.

Recessed Edge Configurations

Similar sightline temperature increases can be obtained for a vacuum glazing mounted in a frame if the edge seal is recessed into the surrounding sash. The vacuum glazing was mounted in a commercially available fixed wood-casement frame, and the edge effect was measured for both conventional flush-mounted and recessed-edge configurations. The window tested was configured with flush mounting on the left jamb and recessed mounting on the right jamb. The test was carried out only for a recess depth of 1.27 cm (0.50 in.), the probable maximum depth that a commercial manufacturer would use. Beyond this depth, the increase in edge surface temperatures would be significantly offset by loss in the vision area of the window resulting from the high-profile sash necessary to achieve greater recess depth, or by reduced structural integrity of the sash if the vision profile remained unchanged. The recessed sash was simulated by adding 1.27 cm (0.50 in.) thick

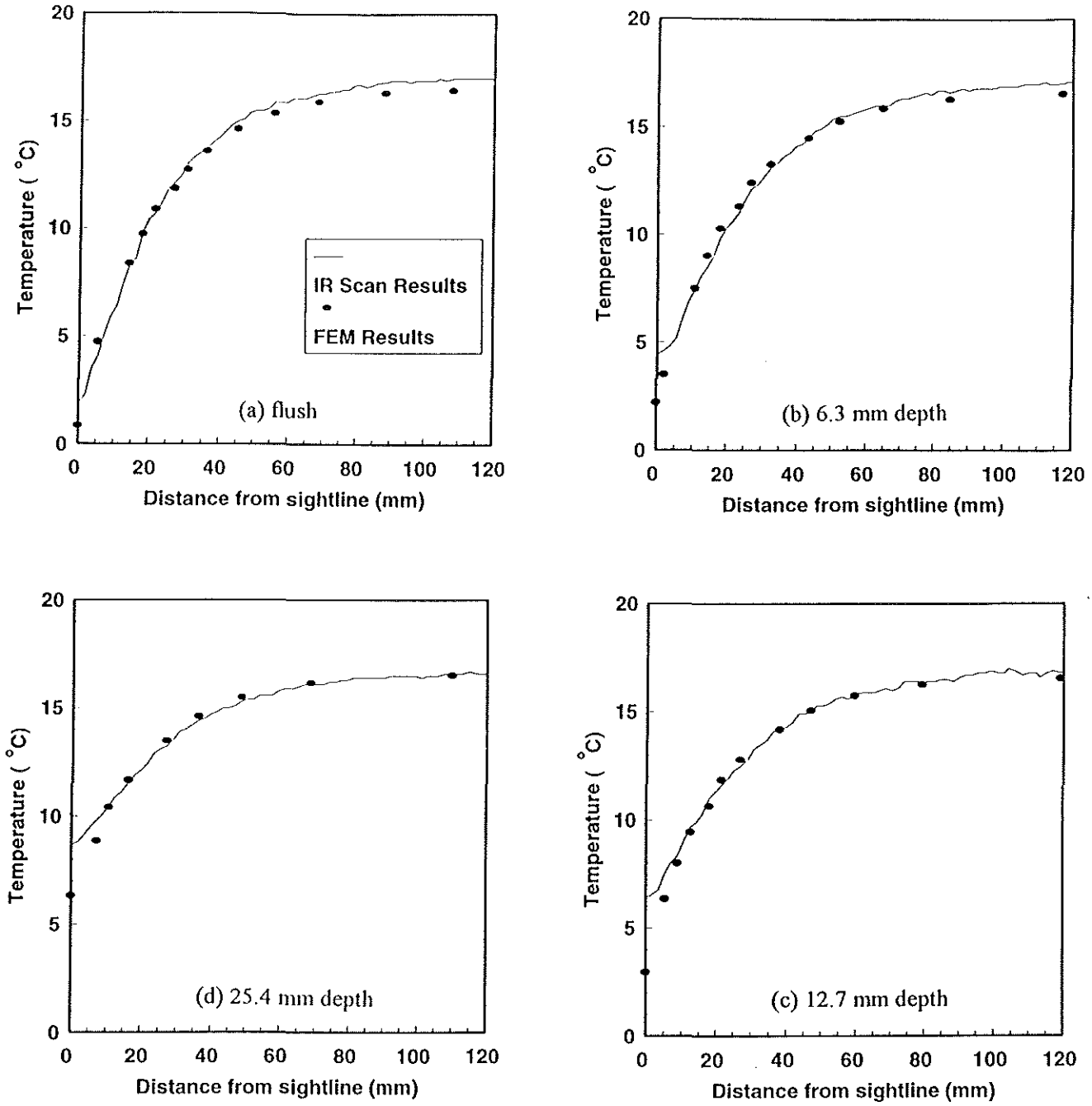

Figure 4 Vacuum glazing edge temperature profiles from infrared (IR) measurements and FEM modeling are compared for different depths of insulation extending past the edge seal sightline. The insulation depth ranges from (a) flush to (d) 25.4 mm (1.0 in.) past the edge seal sightline.

wood strips to both the warm and cold sides of the glazing. The measured sightline temperature of the recessed side was 5.1 C (9.2 F) warmer than that of the nonrecessed side. However, recessing the glazing edge into the sash resulted in a minimum sash surface temperature 0.7 C (1.3 F) lower than that of the sash surface on the nonrecessed side. For comparison, the conventional atmospheric pressure superwindow (not shown) was also mounted and tested in the wood casement frame. Temperature profiles from these tests are plotted in Figure 5.

Addition of a Low-e Third Pane

The extreme of insulating or recessing an edge seal to mitigate edge effects would be to cover the edge region entirely. As shown in Figure 4, the edge region is shifted along the glass as more insulation is added. Completely eliminating the edge effect would necessitate covering the entire vacuum glazing with a highly insulating third layer. To simulate this condition, a third pane of low-emissivity (low-e) glass was added to the sash, completely covering the warm-side surface of the vacuum

glazing. The emissivity of the low-e coating is 0.2. The low-e pane was separated from the vacuum glazing by 1.27 cm (0.50 in.) thick wood glazing stops, creating a 1.27-cm air cavity between the vacuum glazing and the third pane. The low-e surface faced the air cavity. As in the previous test, each side of the window had a different configuration; the left jamb glazing stops were flush with the edge-seal sightline, and the right jamb edge seal was recessed by 1.27 cm (0.50 in.) into the sash as before

Temperature profile results from the IR tests are shown in Figure 5, and the IR data are summarized in Table 1. The edge effect was still present because of thermal bridging through the frame and the wood spacer; however, it was reduced significantly by the addition of the wood-spaced, low-e third pane. With the addition of the third pane, the sightline temperature for the flush.

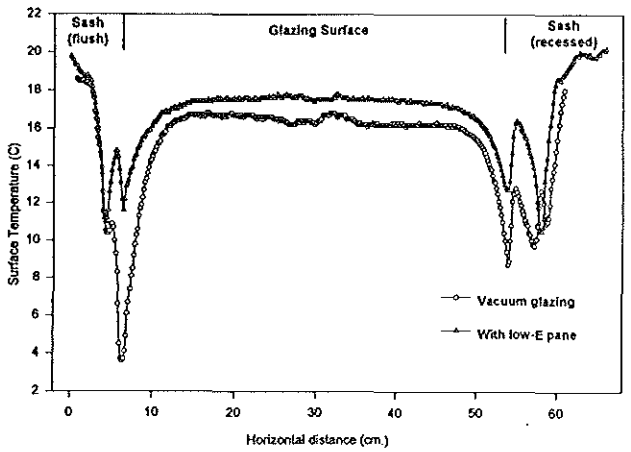

Figure 5 Thermographic measurements of warm-side surface temperatures for a vacuum glazing with and without the addition of a third low-e pane. The glazings were mounted in a fixed wood casement frame with the glazing spacer flush to the sightline on the left side, and recessed by 12.7 mm (0.50 in.) on the right side.

Table 1

	Vacuum Glazing (°C)	Vacuum Glazing with Additional Low-e Pane (°C)
Sightline (flush edge)	3.6	11.6
Sightline (recessed edge)	8.7	12.7
Center-of-glass (flush edge)	16.5	17.5
Center-of-glass (recessed edge)	16.5	17.5
Sash, minimum (flush edge)	10.4	11.0
Sash, minimum (recessed edge)	9.7	10.5

edge configuration increased by 8.0 ℃ (14.4 ℉), the sightline temperature for the recessed edge configuration increased by 4.0 ℃ (7.2 ℉), and the average center-of-glass temperature increased by 1.0 ℃ (1.8 ℉). Minimum sash temperatures are lower than sightline temperatures for the third pane because of the effect of the cold glazing edge behind the wood spacers. This effect could be reduced with the use of a more insulating spacer material between the vacuum glazing and the third pane. The need for a recessed glazing edge is virtually eliminated by the use of the third pane; the data show that with the third pane the flush and recessed sightline temperatures are much closer to the center-of-glass temperature than without the third pane, and are within 1.1 ℃ (2.0 ℉) of each other.

MODELING

Heat transfer through the glazing edge was modeled for a given set of environmental conditions using two different methods: (1) a one-dimensional analytical model was solved numerically using finite-difference techniques and (2) a commercial three-dimensional FEM (G+D 1993) was used to model the glazing edge. To compare modeling results with experimental results, the same environmental conditions and physical properties of the vacuum glazing were used in each model as those used in the infrared thermography. The modeled and tested glazing consists of two sheets of 4-mm glass with low-emittance coatings, a gap width of 0.2 mm, and a sheet and solder glass thermal conductivity of 1.0 W/m K. The gap conductance is specified to be 1.2 $W/m^2 K$, as measured experimentally using a guarded hot-plate apparatus (Collins et al. 1993). Of this conductance, 0.8 $W/m^2 K$ is due to radiative heat transfer and 0.4 $W/m^2 K$ is due to pillar conduction.

Analytic Model

The complete analysis of heat flow near the edges of vacuum glazing requires the solution of a set of coupled three-dimensional equations. A simplified, one-dimensional model has been developed with only one spatial variable—the distance, x, along the glass sheets. The analysis involves a calculation of the rates of heat flow to the internal and external surfaces of the glass sheets by convection and radiation, and along the glass sheets by conduction. The basic assumption in the model is that the temperature of the glass is uniform throughout the thickness of the sheets, and that temperature gradients exist only along the x-axis of the sheets. As will be shown, this assumption is justified by the good agreement between the results obtained with this simple one-dimensional model and a full three-dimensional one. For a glazing with two sheets of low-emittance glass, the temperature gradient through the glass sheets is only about 0.03°C/mm.

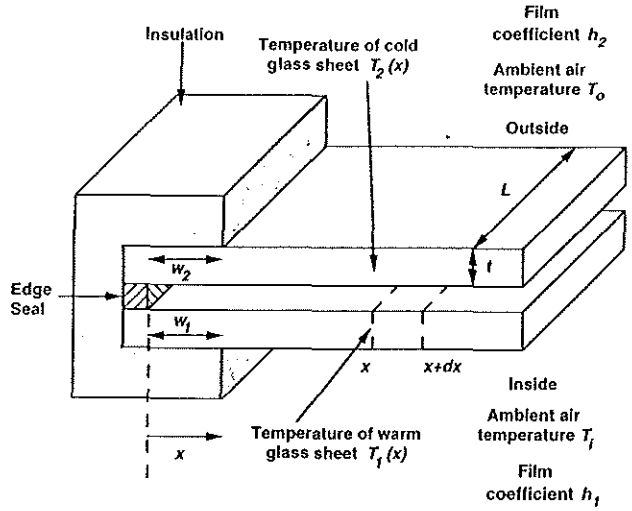

Figure 6 *Schematic diagram of edge region for analytic model.*

The specific geometry to be considered is shown in Figure 6. Two sheets of glass, each of thickness t, width L, and thermal conductivity λ, are joined at their edges by a solder glass seal. Between the two sheets is a high vacuum (< 0.1 Pa). The dominant modes of heat transfer in this gap are radiative transfer between the glass sheets and thermal conduction through the support pillars. The bottom sheet is exposed to a higher ambient temperature, T_i, than the top sheet, where the ambient temperature is T_o. Convective heat transfer occurs over the glass surfaces; thus, the temperatures at these surfaces, $T_1(x)$ and $T_2(x)$ on the warm and cold sides, respectively, are not uniform. The total heat transfer to and from the ambient is governed by the film coefficients h_1 and h_2; the film coefficient is defined as the sum of the convective and radiative heat transfer coefficients. The region around the edge seal is insulated over distances w_1 and w_2 on each side.

The heat flow through each mechanical support pillar in the glass sheets is highly three-dimensional close to the pillar and mostly one-dimensional and highly dependent on the distance away from the pillar. This heat flow is quite uniform at the external surface of the glass sheets, leading to typical point-to-point variations of less than 10% of the temperature difference between the air and the surface. Therefore, the array of pillars can be considered as a slab of material of uniform thermal conductivity. The heat flow through the pillars can then be determined from an internal heat transfer coefficient (Collins et al. 1991). The pillar conductance is given by

$$h_{pillar} = 2\lambda a/d^2 \tag{1}$$

where λ is the conductivity of the glass, a is the pillar radius, and d is the pillar separation distance.

If the temperature difference between the two glass sheets is not too large, the radiative heat transport through the vacuum gap also can be determined from a radiative heat transfer coefficient:

$$h_{rad} = 4\sigma\varepsilon_{eff}T^3 \tag{2}$$

where σ is the Stefan-Boltzmann constant, ε_{eff} is the effective emissivity of the two internal glass surfaces, and T is the average of the temperatures of the two glass sheets (far from the edge). It has been shown that the temperature nonuniformities on the inner surface of the glass sheets, because of the local short-circuiting effect of the support pillars, have a negligible effect on the overall radiative heat flow (Collins et al. 1991).

With the above approximations, the internal heat transfer coefficient for the vacuum gap, h_{int}, can be written as

$$h_{int} = h_{pillar} + h_{rad}. \tag{3}$$

Consider a cross-sectional element of the warm-side glass sheet from x to $x + dx$ in the noninsulated region (see Figure 6). The modes of heat flow into this element are as follows:

1. Conductive heat flow along the glass sheet into the element at x: $Q_{cond}(x)$.
2. Conductive heat flow along the glass sheet into the element at $x + dx$: $Q_{cond}(x + dx)$.
3. Heat flow by internal processes (radiation and conduction through the support pillars: dQ_{int}.
4. Heat flow by external convection and radiation from the ambient at temperature T_i to the surface of the element: dQ_{ext}.

If heat flow into the element is defined as positive, these modes of heat transfer are governed by the following equations:

$$Q_{cond}(x) = -\lambda tL\left.\frac{dT_1(x)}{dx}\right|_x \tag{4}$$

$$Q_{cond}(x+dx) = \lambda tL\left.\frac{dT_1(x)}{dx}\right|_{x+dx} \tag{5}$$

$$dQ_{ext} = h_1 L dx\,[T_i - T_1(x)] \tag{6}$$

$$dQ_{int} = -h_{int} L dx\,[T_1(x) - T_2(x)]. \tag{7}$$

Applying an energy balance to the element yields the following differential equation:

$$\left(\frac{\lambda t}{h_1 + h_{int}}\right)\frac{d^2T_1(x)}{dx^2} - T_1(x) + \left(\frac{h_1 T_i + h_{int} T_2(x)}{h_1 + h_{int}}\right) = 0. \tag{8}$$

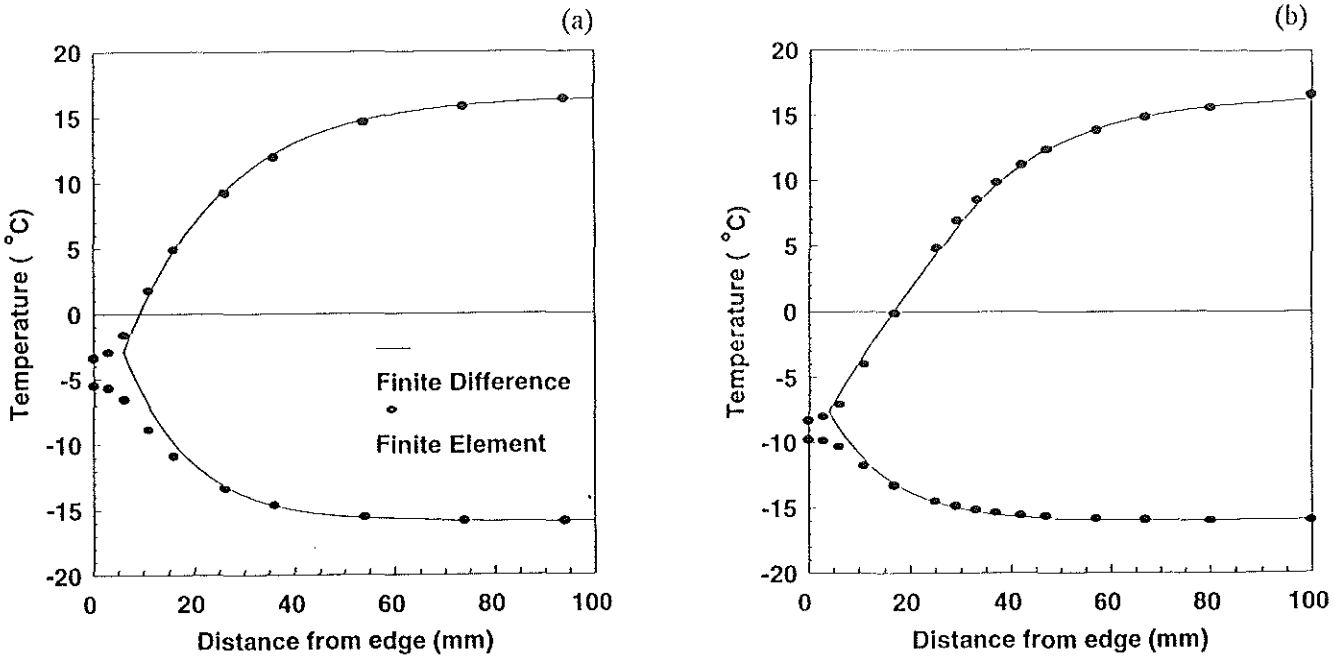

Figure 7 Finite difference and finite element modeling results for a vacuum glazing with (a) an uninsulated edge seal, and (b) an insulated edge seal.

A similar analysis for an element in the noninsulated region on the cold-side sheet (see Figure 6) yields the following differential equation:

$$\left(\frac{\lambda t}{h_2 + h_{int}}\right)\frac{d^2T_2(x)}{dx^2} - T_2(x) + \left(\frac{h_2 T_o + h_{int} T_1(x)}{h_2 + h_{int}}\right) = 0. \quad (9)$$

These coupled differential equations for the two glass surface temperatures can be rewritten in finite-difference form and solved numerically. The boundary conditions are $T_1(0) = T_2(0)$ and $Q_1(0) = Q_2(0)$. Insulated surfaces can be modeled by setting h_1 and h_2 to give an appropriate thermal conductance—zero if the surfaces are assumed to be adiabatic. The finite difference solution for heat transfer through an uninsulated vacuum glazing edge is shown in Figure 7a.

In certain simple cases, Equations 8 and 9 can be solved exactly. Considering exact solutions provides useful insights into the physical processes that determine the rate of heat transfer near the edges of the glazing. In addition, the results derived in these simple cases are useful in estimating external heat transfer coefficients.

The simplest case to consider is perfectly insulating glazing, $h_{int} = 0$. Then Equations 8 and 9 can be decoupled, and the temperature on each side of the glazing given by

$$T_i - T_1(x) = (T_i - T')\exp\left(-x/\sqrt{\lambda t/h_1}\right) \quad (10)$$

and

$$T_2(x) - T_o = (T' - T_o)\exp\left(-x/\sqrt{\lambda t/h_2}\right) \quad (11)$$

where T' is derived from applying continuity of heat transfer at $x = 0$ and is

$$T' = \frac{\sqrt{h_1}T_i + \sqrt{h_2}T_o}{\sqrt{h_1} + \sqrt{h_2}}. \quad (12)$$

In this simple case, the temperature approaches its center-of-glazing value exponentially with a characteristic distance of

$$l = \sqrt{\lambda t/h} \quad (13)$$

where h is the appropriate external heat transfer coefficient. For this case, the additional heat flow from edge effects, per unit length of the edge, is

$$Q_{edge} = \frac{(T_i - T_o)\sqrt{\lambda t}}{h_1^{-1/2} + h_2^{-1/2}}. \quad (14)$$

A second case that can be solved exactly is for a perfectly insulating sample with uninsulated edges extending distances of w_1 and w_2 from the edge. In this case, the temperature varies exponentially along the glass in the uninsulated regions with the same characteristic distance as given in Equation 13, and linearly in the insulated region.

For a specimen that is not perfectly insulating, an approximate solution can be obtained in the symmetrical case of equal heat transfer coefficients on both warm and cold sides, provided that heat transfer between the

sheets in the externally insulated region is neglected. In this case, simple exponential temperature dependencies occur in the uninsulated region, with a characteristic distance given by Equation 13, where $h = h_{ext} + 2h_{int}$.

Three-Dimensional Finite-Element Model

A three-dimensional finite-element model (FEM) of a vacuum glazing was constructed using a commercially available code (G+D1993). Because the four quadrants of the glazing are identical, it is necessary to model only a quarter section of a full window. All of the FEM results presented here lie along the edge of the quarter pane, i.e., the centerline of the full glazing. The external heat transfer to ambient on each side is modeled as conduction through a slab of specified thickness and conductivity to obtain an equivalent film coefficient. This approach ignores the complicating effects associated with convection, which can lead to a vertical temperature gradient across the glazing. Thermographic measurements of the warm-side surface of the vacuum glazing show that, apart from the edge effect, the surface temperature of the entire center-of-glass region is nearly uniform. Thus, the fact that the FEM ignores convective effects external to the glazing should not be a concern in comparing FEM modeling to the experimental tests. External insulation also is modeled as a slab with a uniform thickness and thermal conductivity.

Comparison of Analytic and Finite-Element Modeling

As shown by Figure 7a, analytic and FEM results agree well, except near the edge. Results at the edge diverge because of different treatments of thermal short-circuiting at the edge seal and its effect on nearby heat flow. The FEM accurately models temperature gradients through the thickness of the glass sheets. The finite-difference model simulates the thermal effects of an edge seal, but cannot simulate temperature variations through the thickness of the glass. Such effects, however, only affect the surface temperatures close to the edge seal.

To test the models further, an insulated edge was considered. Figure 7b is a plot of modeling results of the vacuum glazing with a 25.4-mm (1.0-in.) width of insulation along the edge of the warm side of the glazing. The asymmetry between the warm- and cold-side temperature profiles is a result of only one side being insulated. Once again, the two sets of modeling results agree closely, except near the edge.

DISCUSSION

The effect of edge spacer conductance on total window U-factors is discussed further by Beck and Arasteh (1992). Because the center-of-glass thermal performance of vacuum glazing is equal to, and theoretically better than, the performance of atmospheric-pressure glazings, mitigation or elimination of vacuum glazing edge effects will help increase the attractiveness of these glazings for the commercial market. In actual applications, vacuum glazings will most likely be installed with some sort of insulated edge configuration, and/or may be used in conjunction with a third low-e glass pane to reduce edge conduction and the resulting thermally induced edge stresses. The third pane option is attractive because it allows use of spectrally selective coatings that cannot withstand the 500 C bake-out temperature of the vacuum glazing. However, the combined mass of the third pane with the two 4-mm-thick glass panes of the vacuum glazing may require structural redesign of conventional operable frames.

A nationally accepted U.S. simulation methodology (NFRC 1991) based on two programs (LBL 1992; EE 1992) has been used to estimate the range of U-factors to be expected for the tests involving the wood-framed glazings for ASHRAE winter conditions and a window size of 91.4 cm by 122 cm (36 in. by 48 in.). One program is a public-domain, one-dimensional, finite-difference-method (FDM) model for simulating heat transfer through glazings and for calculating total U-factors for fenestration products. The other is a commercially available two-dimensional FDM model for simulating heat transfer through the frame and edge-of-glass regions of fenestration products. These two programs were used in

Table 2

	COG	U-Factor, EDGE	$W/m^2 \cdot K$ FRAME	TOTAL	Sightline Temp. °C
Vacuum glazing, flush edge	1.00	2.09	2.23	1.52	–2.3
Vacuum glazing, recessed edge	1.00	1.58	2.07	1.42	6.0
Vacuum glazing, flush edge, low-e third pane	0.75	1.52	1.69	1.14	8.8
Vacuum glazing, recessed edge, low-e third pane	0.75	1.32	1.71	1.14	10.0
Superwindow, flush edge	0.68	1.06	1.65	1.01	10.0
Superwindow, recessed edge	0.68	0.87	1.57	0.99	13.2

combination to model the heat transfer through the vacuum glazing and the superwindow and to calculate U-factors for the frame, edge, and total window. The results are summarized in Table 2.

CONCLUSIONS

Edge effects resulting from thermal bridging through the edge seal of vacuum glazings are significant and can cause reduced condensation resistance and higher total window U-factors than are found in conventional high-thermal-performance glazings with thermally broken spacers.

The center-of-glass performance of vacuum glazings currently is lower than that of state-of-the-art superwindows (which can achieve center-of-glass U-factors on the order of 0.45 $W/m^2 \cdot K$ [0.08 $Btu/h \cdot ft^2 \cdot °F$] using xenon fills). With mitigation of edge effects, total window performance of vacuum glazings should be comparable to or better than that of superwindows.

Computer modeling indicates that with the addition of a third low-e pane, the vacuum glazing has a total window U-factor 13% higher than that of a state-of-the-art superwindow. It also indicates that for the third pane configuration, recessing the glazing edge does not change the total window U-factor appreciably.

Coatings with lower emissivity than the one used in this vacuum glazing, that can withstand the high-temperature manufacturing process, would improve the thermal performance of the vacuum glazing.

The results of the analytical and FEM models used in this paper are in good agreement with each other and with the IR measurements; in other words, edge effects in vacuum glazings can be modeled accurately using analytic and FEM techniques.

ACKNOWLEDGMENTS

This work was supported by His Royal Highness Prince Nawaf bin Abdul Aziz of the Kingdom of Saudi Arabia through the Science Foundation for Physics at the University of Sydney, by the Australian Energy Research and Development Corporation, and by the Assistant Secretary for Energy Efficiency and Renewable Energy, Office of Building Technologies, Building System and Materials Division of the U.S. Department of Energy under contract no. DE-AC03-76SF00098. The authors wish to thank Scot Miller and Marlo Van Klompenberg at Pella Corporation and Tom Pass at Southwall Technologies for their donation of test materials for this project.

REFERENCES

Arasteh, D., F. Beck, B. Griffith, M. Acevedo-Ruiz, and N. Byars. 1992. Using infrared thermography for the study of heat transfer through building envelope components. *ASHRAE Transactions* 98(1): 819-824.

ASTM. 1991. ASTM C 1199, Standard test method for measuring the steady state thermal transmittance of fenestration systems using hot box methods. *Annual Book of ASTM Standards*, vol. 04.06, pp. 671-682. Philadelphia, Pa.: American Society for Testing Materials.

Beck, F.A., and D. Arasteh. 1992. Improving the thermal performance of vinyl-framed windows. *Proceedings of the ASHRAE/DOE/BTECC Conference on the Thermal Performance of the Exterior Envelopes of Buildings V*, Clearwater Beach, Fla. Also published as Lawrence Berkeley Laboratory Report LBL-32782, October 1992, Berkeley, Calif.

Byers, N., and D. Arasteh. 1990. Design options for low-conductivity window frames. LBL Report LBL-30498. Berkeley, Calif.: Lawrence Berkeley Laboratory.

Collins, R.E., C.J. Davis, C.J. Dey, S.J. Robinson, J.-Z. Tang, and G.M. Turner. 1993. Measurement of local heat flow in flat evacuated glazing. *Int. J. Heat Mass Transfer* 36: 2553-2563.

Collins, R.E., L. Poladadian, B.A. Palthorpe, and R.C. McPhredan. 1991. Heat conduction through support pillars in evacuated windows. *Aust. J. Phys.* 44: 73-86.

Collins, R.E., A.C. Fisher-Cripps, and J.-Z Tang. 1992. Transparent vacuum insulation. *Solar Energy* 49(5): 333-350.

EE. 1992. FRAME—A computer program to evaluate the thermal performance of window frame systems, version 3.0. Waterloo, Ont.: Enermodal Engineering Ltd.

Fisher-Cripps, A.C., R.E. Collins, G.M. Turner, and E. Bezzel. 1995. Stresses and fracture probability in evacuated glazing. *Building and Environment* 30(1): 41-59.

Frost, K., D. Arasteh, and J. Eto. 1993. Savings from energy efficient windows: Current and future savings from new fenestration technologies in the residential market. LBL Report LBL-33956. Berkeley, Calif.: Lawrence Berkeley Laboratory.

Garrison, J.D., and R.E. Collins. 1995. Manufacture and cost of vacuum glazing. *Solar Energy.* In press.

G+D. 1993. STRAND6, finite element analysis system. Sydney, Australia: G+D Computing Pty. Ltd.

Griffith, B.T., F.A. Beck, D.K. Arasteh, and D. Türler. 1995. Issues associated with the use of infrared thermography for experimental testing of insulated systems. *Proceedings of the Conference on the Thermal Performance of the Exterior Envelopes of Buildings VI*, Orlando, Fla., December 5-8.

LBL. 1992. WINDOW 4.0—A PC program for analyzing the thermal performance of fenestration products. LBL-32091. Berkeley, Calif.: Windows and Daylighting Group, Lawrence Berkeley Laboratory.

NFRC. 1991. *NFRC 100-91, Procedure for determining fenestration product thermal properties (currently limited to U-values).* Silver Spring, Md.: National Fenestration Rating Council.

Robinson, S.J., and R.E. Collins. 1989. Evacuated windows—Theory and practice. *ISES Solar World Congress*. Kobe, Japan: International Solar Energy Society.

Simko, T.M., R.E. Collins, A.C. Fisher-Cripps, and J.D. Garrison. 1995. An overview of the technology of vacuum glazing. *Proceedings of the Window Innovations Conference '95*. June 5-6. Toronto, Ont., Canada. In press.

Zoller, F. 1924. Hollow pane of glass. German Patent No. 387 655.